



Joint Institute for Nuclear Research
Dzhelepov Laboratory of Nuclear Problems

Radiation Protection and the Safety of Radiation Source

Final Report- START Programme

Supervisor: Dr. Said Abou El-Azm

Marina Romani Abdelnour
Ain Shams University, Egypt

Tarek Mohamed M Hammam
South Valley University, Egypt

Participation period: January 22 – March 4, 2023

Dubna, 2023

Contents

1	Introduction	3
2	Materials and Methods	4
2.1	Sample Preparation	4
2.2	Sample Irradiation	4
2.3	Sample Measurements	4
2.3.1	X-123 CdTe Detector	4
2.3.2	GaAs pixel Detector	5
3	Results	5
3.1	Detection Energy Calibration Curve of the CdTe Detector	6
3.2	Studying the Registration Efficiency of CdTe Detector	6
3.3	Calculation of the Real Spectrum of CdTe Detector	7
3.4	Characteristic of X-Ray Tube Using CdTe Detector	7
3.5	Separation of Iodine and Different Elements Using a CdTe Detector at Various Concentrations	8
3.6	Studying the Characteristics of a GaAs Pixel Detector Using Different Al Foil Thicknesses	11
3.7	Studying the Characteristics of a GaAs Pixel Detector at Different Currents	11
3.8	Studying the Characteristics of a GaAs Pixel Detector at Different Bias-Voltages	12
3.9	Identification of Human Elements Using a GaAs Pixel Detector	13
4	Conclusion	14

Summary

Separation of more than two types of materials, such as iodine, lanthanum, and gadolinium, that resemble soft tissue, is possible with X-ray computed tomography (CT), using semiconductor detectors. As a result, we investigated in this study how to use the X-123 CdTe detector and the GaAs pixel detector to distinguish between various materials and their concentrations. We also aimed to study the characteristics of GaAs pixel detectors under varying current and bias voltages, utilizing various thicknesses of aluminum foil. Our experimental measurements took place in the JINR Dzheleпов Laboratory of Nuclear Problems in Dubna, Russia.

1 Introduction

Medical imaging techniques (Fig. 1) are a crucial method to examine the inside of the body without making a surgical incision. Imaging is no longer only used for medical diagnosis, but is increasingly vital for image-guided therapies. Moreover, cutting-edge imaging methods are being used to investigate systemic activities including flow rates, oxygen concentrations, and metabolism. Medical imaging is classified into two types: interventional imaging and diagnostic imaging. Interventional imaging includes angiography, fluoroscopy, endoscopy and laparoscopy. While diagnostic imaging includes X-rays, magnetic resonance imaging (MRI), ultrasound, computed tomography (CT), and nuclear medicine. Due to the rapid development of more precise, less intrusive, and faster equipment during the past ten years, medical imaging has undergone a revolution. Therefore, the design of a medical imaging system has to take into consideration all the requirements that can be derived from analyzing the desired applications. Many parameter requirements have to be addressed, including type of detectors, detector size, and contrast resolution [1, 2].

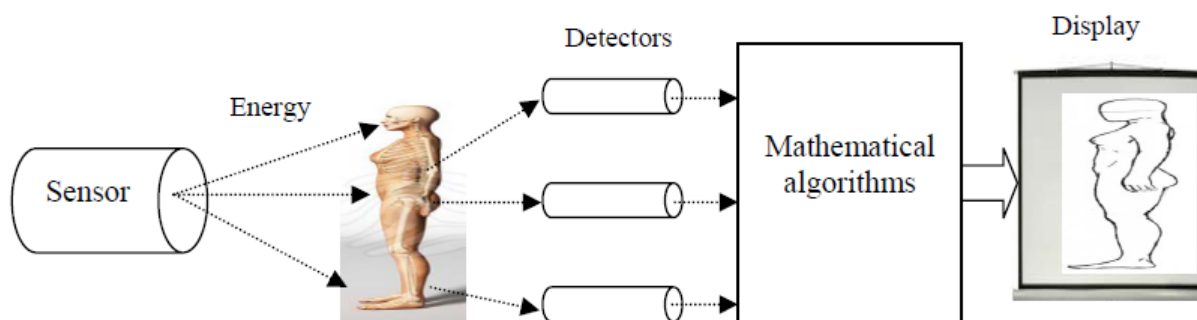


Fig. 1: Medical imaging system [3].

In the past few years, semiconductor nuclear radiation detectors have advanced significantly. Currently, they are used in a wide range of industries, nuclear sciences, high energy physics, astronomy and nuclear medicine. Compared to other types of detectors, such as scintillators and gas detectors, semiconductor detectors provide good energy resolution, imaging capabilities, and the flexibility to fabricate small systems. They are also more sensitive that enables them to minimize the radiation exposure of computed tomography. The most promising compounds for semiconductor radiation sensors are cadmium telluride (CdTe) and gallium arsenide (GaAs) due to their outstanding high detection efficiencies, energy resolution and room temperature functioning [4–6].

2 Materials and Methods

2.1 Sample Preparation

Firstly, we used standard sources for calibration, including Co-57, Co-60, Cs-136, and Am-241. We also used different types of materials with K-edges in the desired energy range, such as those that resemble soft tissue (e.g., I, Gd, La, Nd and bone). we prepared the previous materials with different concentrations. The concentrations are I (25-100%), Gd (100%) La (80%), and Nd (20%).

2.2 Sample Irradiation

The X-ray tube was generated at 80 kVp as illustrated in (Fig. 2)

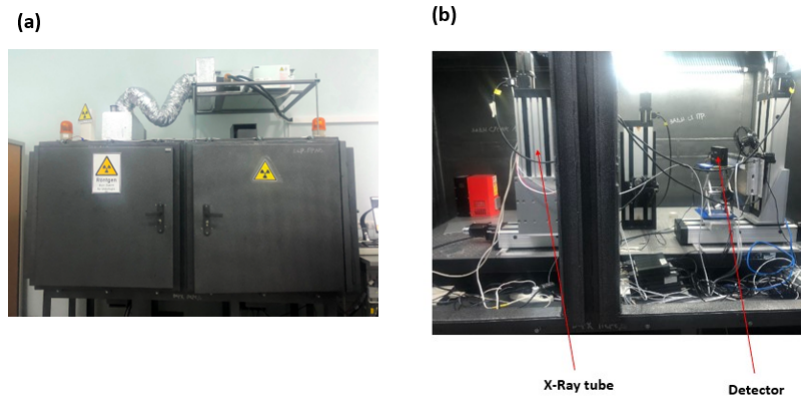


Fig. 2: (a) Shows the system from outside. (b) Shows the system from inside.

2.3 Sample Measurements

The detectors used in the experiment were CdTe and GaAs as illustrated in (Fig. 3) and (Fig. 4). The detectors are capable of detecting X-rays up to 120 kVp. The CdTe detector is a 1mm diameter and the complete system is packaged in $7 \times 10 \times 2.5 \text{ cm}^3$ aluminum and collimator with 80 kVp. While GaAs detector is 300 μm . The size of detector $1.5 \times 1.5 \text{ cm}^2$ and the distance from X-ray source to the detector is 40 cm.

2.3.1 X-123 CdTe Detector

The X-123 CdTe detector is a typical type of X-ray detector used in high-resolution X-ray imaging applications, such as medical imaging. The material used to construct it is CdTe, a semiconductor that is susceptible to X-rays and other high-energy radiation. The X-123 CdTe detector is designed to provide high-resolution X-ray images with remarkable contrast and sensitivity. It is recognized for having less noise and fast response times, which makes it ideal for applications needing real-time imaging. The X-123 CdTe detector is a popular choice for medical imaging applications like mammography, where the ability to identify tiny tumors with great precision is necessary for early diagnosis and treatment.



Fig. 3: Shows X-123 CdTe detector.

2.3.2 GaAs pixel Detector

GaAs pixel-type radiation detectors are commonly used in particle physics research. Its fabrication uses the semiconductor material GaAs, which is sensitive to high-energy particles like gamma rays and X-rays. The detector is made up of a grid of small pixels, that have the ability to distinguish between different particles and report on their position and energy. GaAs pixel detectors are recognized for their exceptional spatial resolution and rapid response times, which make them ideal for applications requiring accurate particle tracking, such as high-energy physics research or medical imaging.



Fig. 4: Shows GaAs Pixel detector.

3 Results

During this project, we used two types of detectors, the X-123 CdTe and GaAs Pixel detectors. Every detector has its characteristics. Therefore, we studied the following properties and each method is explained in detail in the following results.

- Calibration curve of detectors
- Studying the registration efficiency of CdTe detector
- Calculation of the real spectrum of CdTe detector
- Characteristic of X-ray tube using CdTe detector
- Separation of iodine and different elements using a CdTe detector at various concentrations
- Studying the characteristics of a GaAs pixel detector using different Al foil thicknesses

- Studying the characteristics of a GaAs pixel detector at different currents
- Studying the characteristics of a GaAs pixel detector at different bias-voltages
- Identification of human elements using a GaAs pixel detector

3.1 Detection Energy Calibration Curve of the CdTe Detector

We used standard sources including Co-57, Co-60, Cs-137, and Am-241 for calibration. We get the calibration curve and equation as shown in (Fig.5).

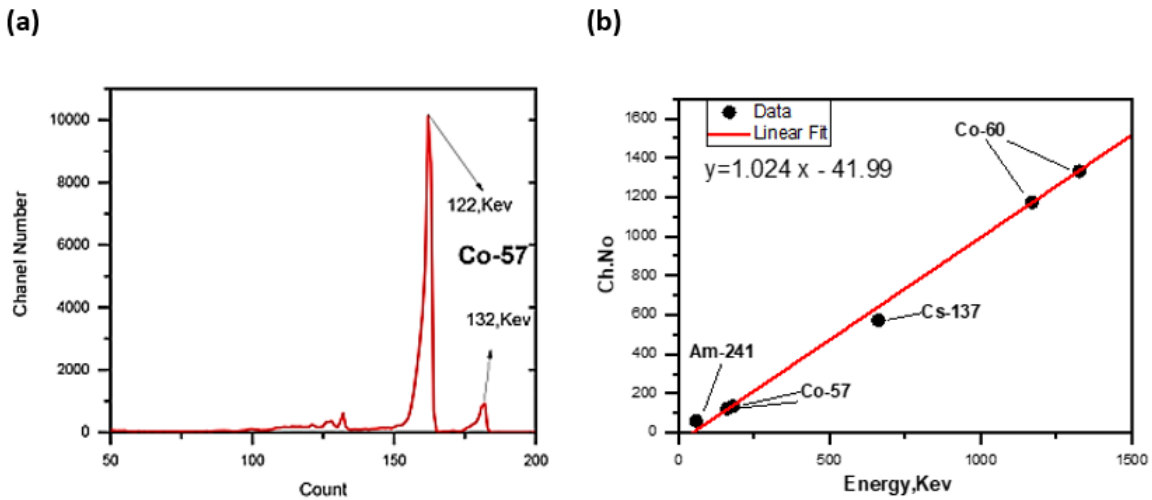


Fig. 5: (a) Shows spectra of Co-57. (b) Shows energy calibration curve for CdTe detector.

3.2 Studying the Registration Efficiency of CdTe Detector

The efficiency of the detector is one of the most crucial features of the detector. The detector count efficiency is related to the amount of radiation emitted from the radiation source to the measured amount of the detection. Important advantages of CdTe are high detection efficiency, performance at room temperature, suitable for the creation of small, and dependable detection systems [4]. Therefore, we have determined the registration efficiency of CdTe detector with a thickness of 1mm as illustrated in (Fig. 6), using [photon cross section database](#). We calculated the registration efficiency using (equation 1).

$$P = 1 - \text{Exp}(-\mu x) \quad (1)$$

Where μ is the mass attenuation coefficient, and x is the thickness of absorbed material.

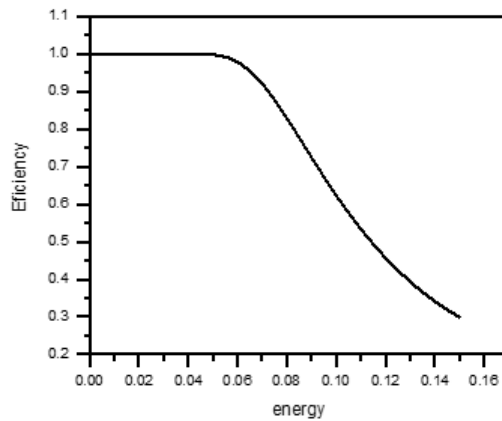


Fig. 6: Shows the registration efficiency of CdTe detector at a thickness 1mm.

3.3 Calculation of the Real Spectrum of CdTe Detector

We calculated the real spectrum of the CdTe detector using pure X-ray spectrum with taken into account 40 cm distance between the X-ray tube and detector. We will get the real spectrum by multiplying the count of the pure spectrum with the efficiency. There is not much of a difference between the spectrum of pure-X ray and real as shown in (Fig. 7).

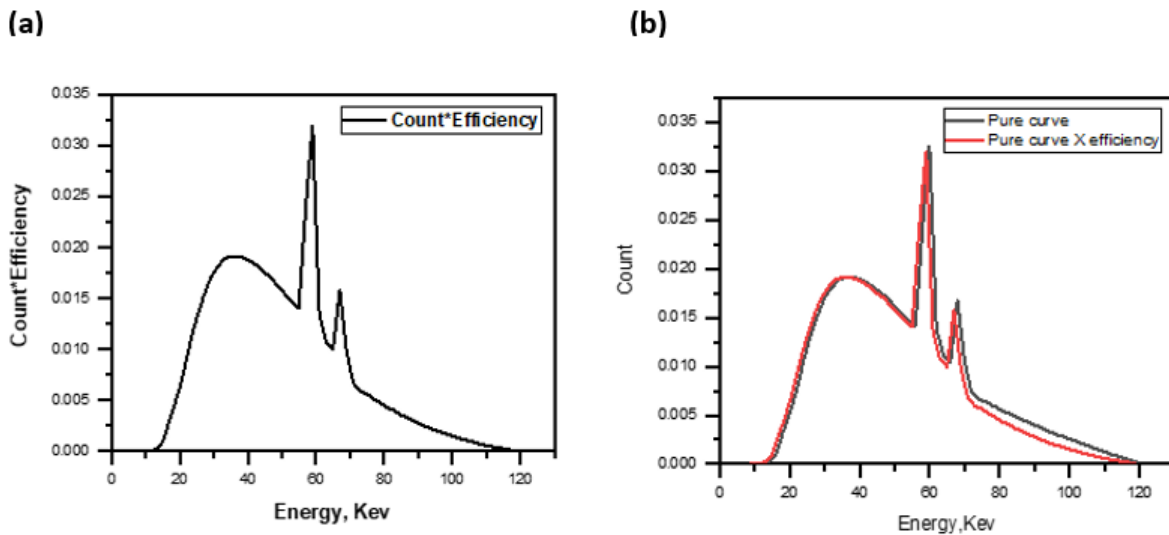


Fig. 7: (a) Shows the real spectrum of the CdTe detector. (b) Shows the difference between Pure curve and efficiency real spectrum curve.

3.4 Characteristic of X-Ray Tube Using CdTe Detector

In order to study the performance of CdTe, we studied the characterization of the X-ray tube using a wide range of applied voltages ranging from 20 up to 120 kVp as illustrated in (Fig. 8). Thus, the

best performance of the X-ray tube is about 80 kVp.

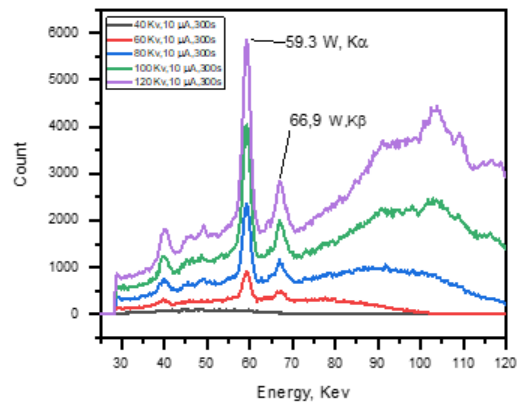


Fig. 8: Shows X-ray characteristic curve at different voltages.

3.5 Separation of Iodine and Different Elements Using a CdTe Detector at Various Concentrations

Four samples with the following iodine concentrations were prepared using standard iodine solutions and distilled water in the following ratios: 1:0, 3:1, 2:2, and 1:3. As indicated in (Fig. 9), we obtained various spectra and compared them to the background spectrum. We can determine iodine edge in every concentration by eliminating background as shown in (Fig. 10).

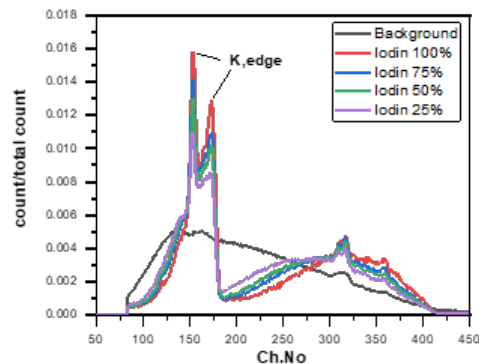


Fig. 9: Shows different concentrations of iodine regarding background.

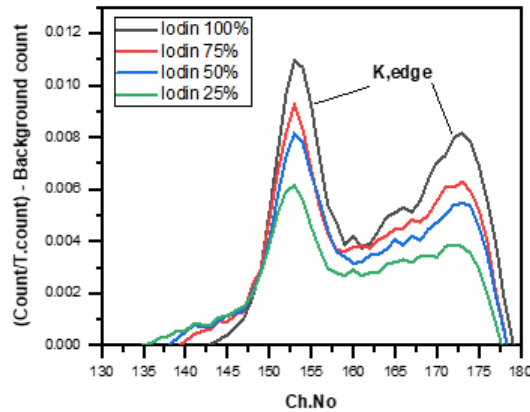


Fig. 10: Shows the edge of different iodine concentrations.

By taking the integration of each edge and drawing a relationship between the value of integration and concentration, we ensured that the detector was effective in differentiating between iodine concentrations. The curve must be a straight line as shown in (Fig. 11), but small variations may occur due to sample preparation conditions.

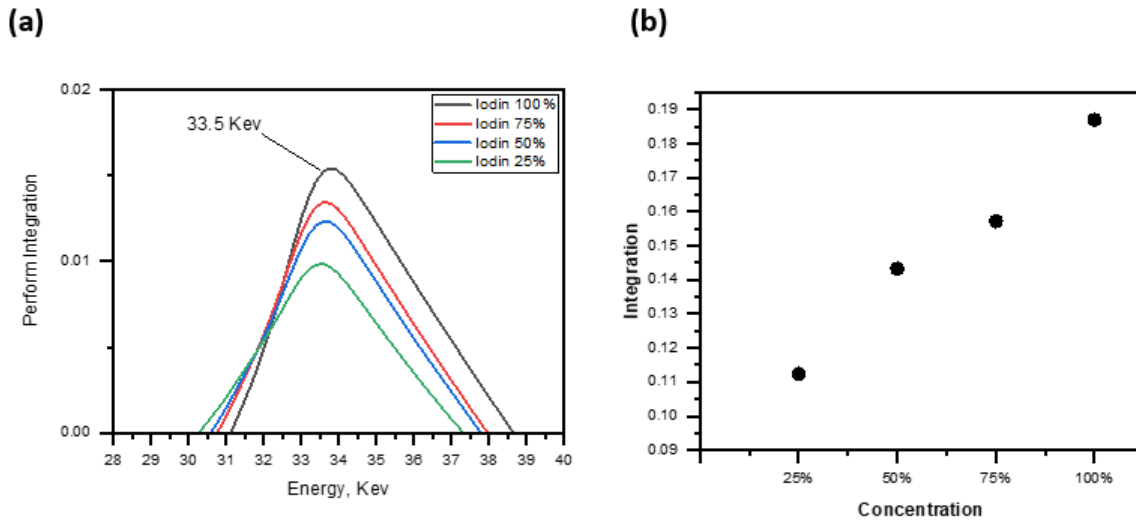


Fig. 11: (a) Shows the perform integration of iodine with different concentrations. (b) Shows the ratio of concentration and k edge of iodine.

Furthermore, we used the CdTe detector to separate various elements such as Gd, and La as shown in (Fig. 12). When X-rays interact with a substance, they have the potential to ionize the atoms that will then lead them to release distinctive X-rays that are unique to the atomic element. Different elements in a sample can be identified and separated by measuring the energy and intensity of these distinctive x-rays using the CdTe detector. We can defined and separate Gd, La

and I from the sample by applying different criteria and by take the integer values of its results as illustrated in (Fig. 13).

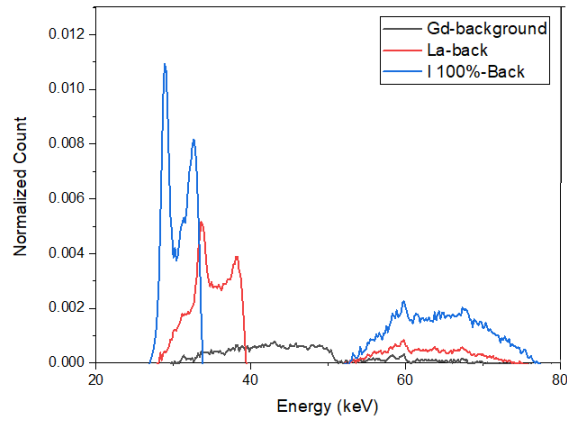


Fig. 12: Shown the energies of gadolinium, lanthanum and iodine in regard to the background before separation.

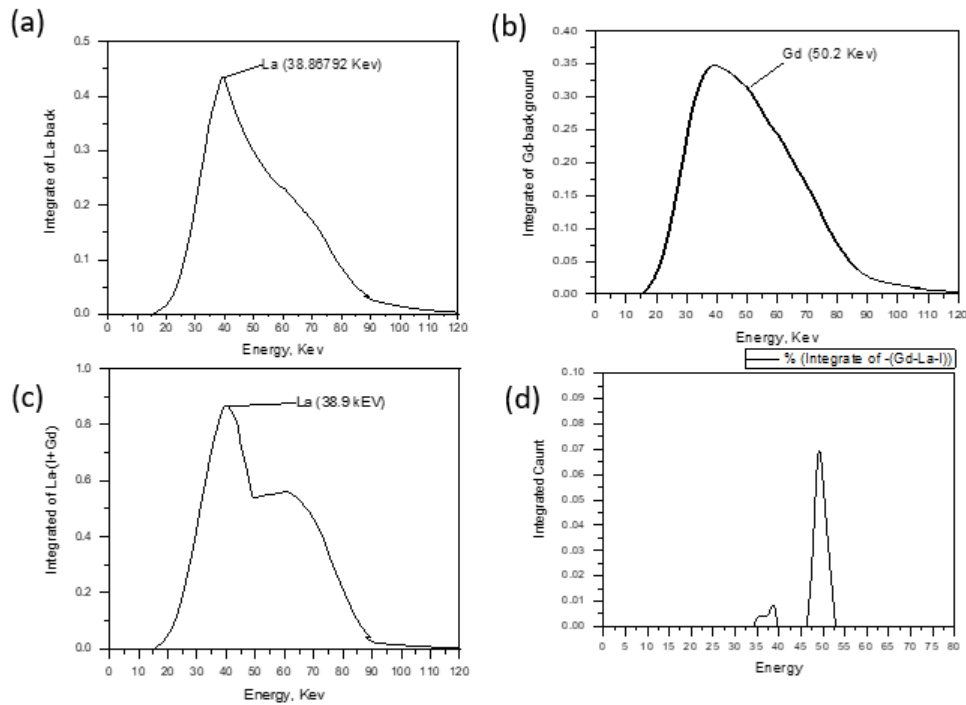


Fig. 13: Shown the energy peak of lanthanum, and gadolinium after calculating the integer of the criteria that applied.

3.6 Studying the Characteristics of a GaAs Pixel Detector Using Different Al Foil Thicknesses

We used various Al foil thicknesses to study the characteristics of the GaAs pixel detector. Furthermore, it is essential to reduce the noise of the X-ray tube. Therefore, we investigated the relationship between The time-over-threshold (TOT) and different foil thicknesses. With increased Al foil thickness, cluster and pixel counts decreased. The most TOT was absorbed by pixels 1 and 2 when an Al foil wasn't used. While using an Al foil with a 16 mm thickness, the TOT absorption was divided throughout various pixels as illustrated in (Fig. 14).

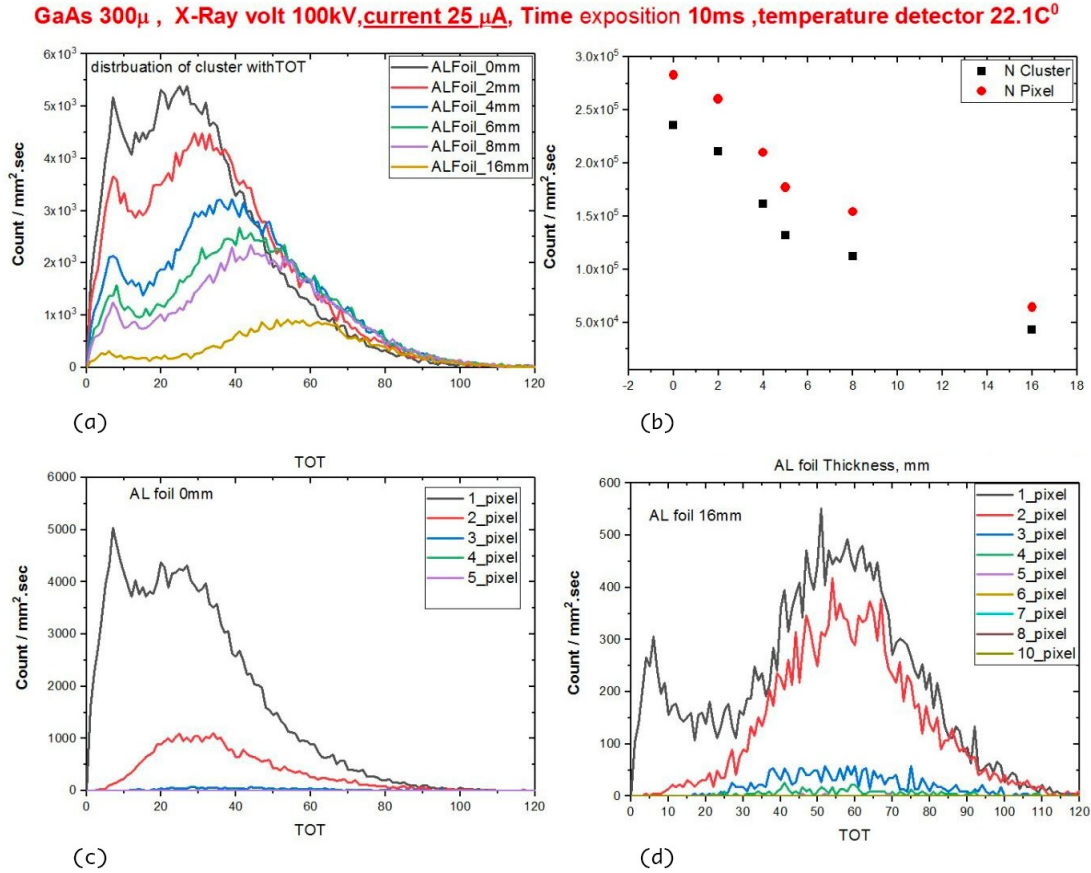


Fig. 14: (a) Shows the relation between TOT with different thicknesses of foils and (b) shows the number of clusters and pixels with increased thickness of foils. (c) Shows the relation between TOT and different number of pixels at AL 0mm and (d) shows the relation between TOT with different number of pixels.

3.7 Studying the Characteristics of a GaAs Pixel Detector at Different Currents

We studied the characteristics of a GaAs pixel detector using a variety of currents to determine the most effective currents for GaAs pixel performance. Subsequently, we determined the number of clusters with increased current, as shown in (Fig. 15). Thus, we investigated the relationship between TOT and various currents ranging from 10 μ A to 150 μ A. When an Al filter with a 4mm

thickness was used, pixels one and two absorb the most TOT at the current 150 μA .

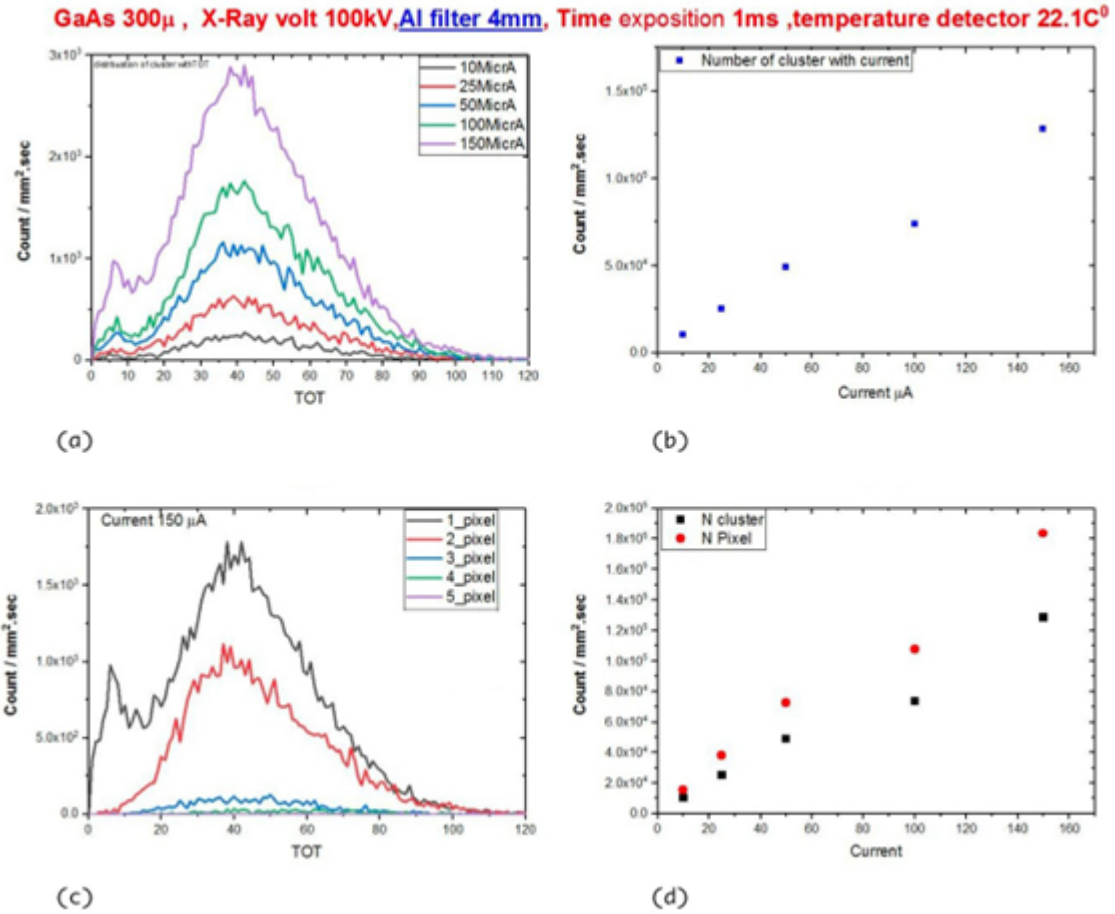


Fig. 15: (a) Shows the relation between TOT with different currents and (b) shows the numbers of cluster with current. (c) Shows the relation between TOT and different number of pixels at 150 μA and (d) shows numbers of pixel and cluster at 150 μA .

3.8 Studying the Characteristics of a GaAs Pixel Detector at Different Bias-Voltages

It is possible to investigate the characteristics of a GaAs pixel detector at different bias voltages to find out more about how it operates and behaves. The bias voltage has a significant impact on the electric field and charge-collection efficiency of the detector. By varying the bias voltage, it is possible to observe how the electric field intensity affects how the detector responds to radiation. Additionally, another significant aspect of a GaAs detector that can be studied in this regard is the number of pixels in a cluster. Increasing the bias voltage can result in an increase in the number of pixels in a cluster because a stronger electric field can improve charge collection and reduce charge sharing between neighboring pixels, as shown in Figure 19(b), at which high voltage we find clusters that contain 6 pixels, but generally the count of clusters that contain 6 pixels is lower than that of clusters that contain more pixels as shown in (Fig. 16).

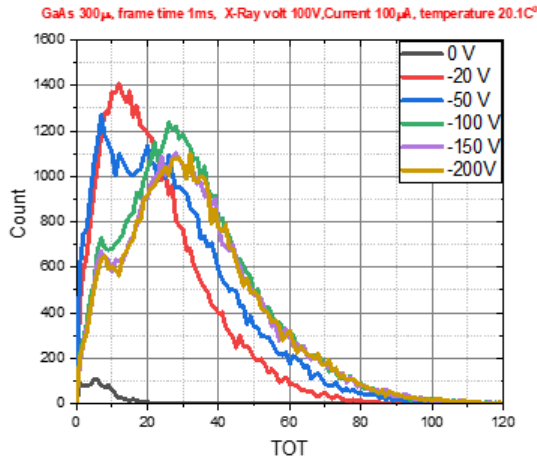
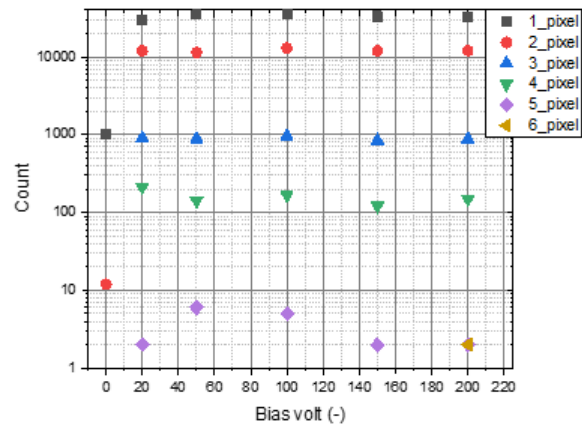
(a)**(b)**

Fig. 16: (a) Shows the relation between TOT with several applied biases. (b) Shows the number of pixels at different bias-voltages.

3.9 Identification of Human Elements Using a GaAs Pixel Detector

We also tried to use the GaAs pixel detector to identify iodine, lanthanum, and gadolinium as illustrated in (Fig.17). we adopt the TOT approach as a measure of the energy deposition [7]. Therefore, the heat maps show the relation between energy and the number of pixels of iodine, lanthanum, and gadolinium while there is a difference in color due to these materials' varied densities.

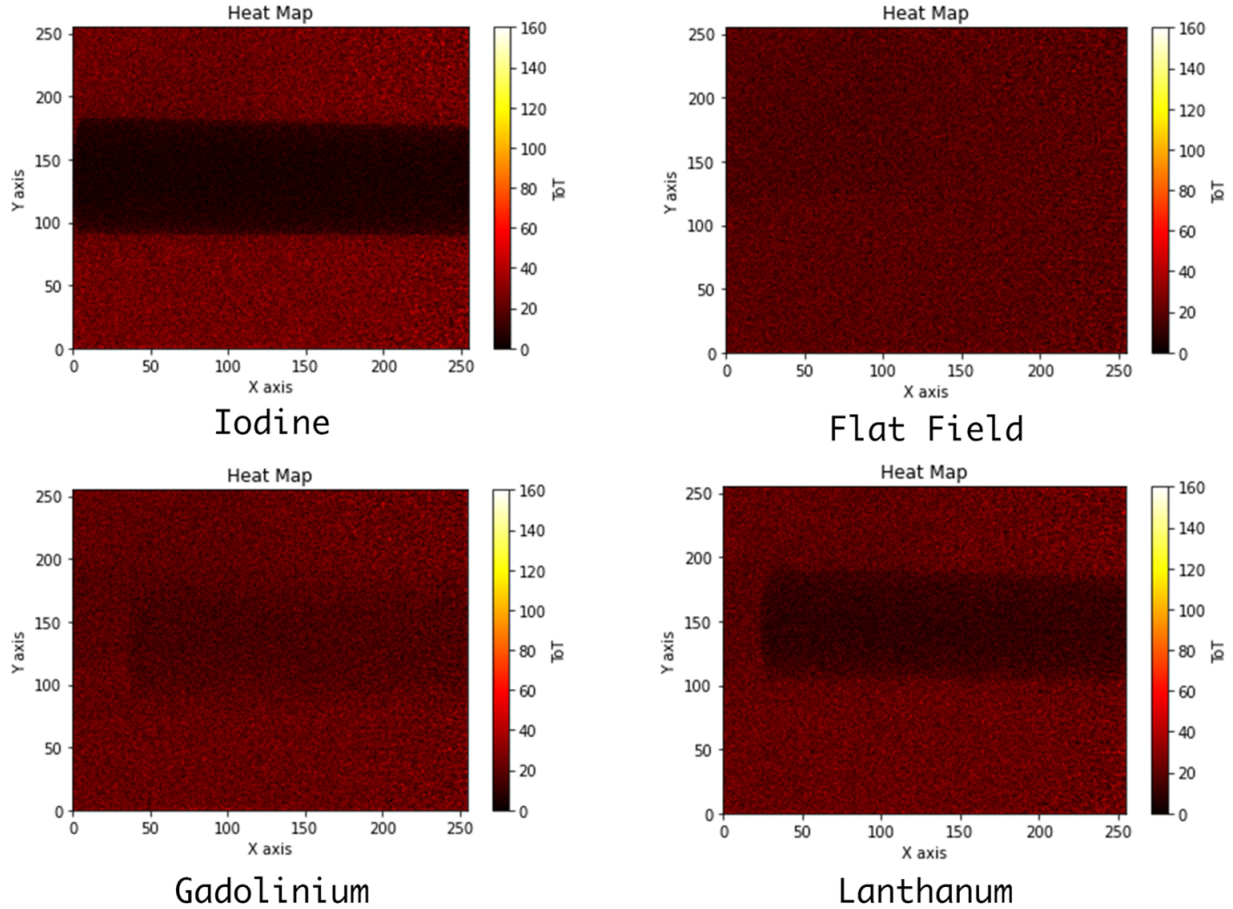


Fig. 17: Shows separation of iodine, lanthanum and gadolinium using GaAs Pixel detector.

4 Conclusion

Semiconductor detectors can be used to separate human materials for medical imaging however, this is not an easy task due to several aspects, such as detector size, contrast resolution, efficiency, and calibration of the detector. Thus, in this project, the CdTe detector and GaAs pixel detector, and their highly favorable properties have been addressed. We were able to identify the ideal image settings needed for accurate material separation utilizing the X-123 CdTe detector and we studied the properties of the GaAs pixel detector.

Acknowledgment

First and foremost, we would like to thank Prof. G. A. Chelkov, the head of the experimental colliding beams section at the DLNP, for his support and gracious welcome. We also like to express our gratitude to Dr. Said Abou El-Azm for his crucial guidance and assistance during this project. He has been a truly great support to us. We additionally wish to express our gratitude to the Joint Institute for Nuclear Research for providing us with the opportunity to participate in this programme. As JINR has been so fulfilling for us, we are very appreciative of everything we have

learned there. Finally, we would like to thank the START programme coordinators, Ms. Olga Korotchik and Ms. Elena Karpova, for their help.

References

- [1] Sigurd Angenent, Eric Pichon, and Allen Tannenbaum. Mathematical methods in medical image processing. *Bulletin of the American mathematical society*, 43(3):365–396, 2006.
- [2] Martin Hoheisel. Review of medical imaging with emphasis on x-ray detectors. *Nuclear Instruments and Methods in Physics Research Section A: Accelerators, Spectrometers, Detectors and Associated Equipment*, 563(1):215–224, 2006.
- [3] Hany Kasban, MAM El-Bendary, and DH Salama. A comparative study of medical imaging techniques. *International Journal of Information Science and Intelligent System*, 4(2):37–58, 2015.
- [4] Stefano Del Sordo, Leonardo Abbene, Ezio Caroli, Anna Maria Mancini, Andrea Zappettini, and Pietro Ubertini. Progress in the development of cdte and cdznte semiconductor radiation detectors for astrophysical and medical applications. *Sensors*, 9(5):3491–3526, 2009.
- [5] Michael Fiederle, Simon Procz, Elias Hamann, Alex Fauler, and Christer Fröjdh. Overview of gaas und cdte pixel detectors using medipix electronics. *Crystal Research and Technology*, 55, 2020.
- [6] GM Lezhneva, RG Melkadze, and LV Khvedelidze. Gaas pixel-detector technology for x-ray medical imaging: a review. *Russian Microelectronics*, 34:229–241, 2005.
- [7] Sushil Sharma, Jyoti Chhokar, Catalina Curceanu, Eryk Czerwiński, Meysam Dadgar, Kamil Dulski, J Gajewski, Aleksander Gajos, M Gorgol, Neha Gupta-Sharma, et al. Estimating relationship between the time over threshold and energy loss by photons in plastic scintillators used in the j-pet scanner. *EJNMMI physics*, 7(1):1–15, 2020.